

# Study on synthesis and electrochemical performance of iron-based compounds for supercapacitor electrode materials

QINGQING ZHANG, SHENGLI XIE\*, JIANXIA GOU\*, QIAN LIU, RUNLONG HUANG, TENG WU  
*Department of Chemical Engineering and Safety, Binzhou University, 391 Huanghefive Road, Binzhou, Shandong 256603, P. R. China*

Supercapacitor is a novel energy storage component which developed in recent years. The electrode material affects the specific capacitance and the cycling stability of the supercapacitor. The emphasis of research is to improve the specific capacity of electrode materials. In this paper, iron-based compounds was successfully prepared respectively by adding sulfosalicylic acid, ammonium fluoride or the mixture of ammonium fluoride and tetrabutyl titanate in the process of synthesis. The iron-based compounds, which was synthesized by ammonium fluoride adding tetrabutyl titanate, had largest capacity  $830 \text{ F g}^{-1}$  at  $1 \text{ A g}^{-1}$ . Simultaneously, the cycling stability with an efficiency of almost 100% after cycling 5000 times at a current density of  $10 \text{ A g}^{-1}$  is achieved.

(Received July 29, 2019; accepted June 16, 2020)

*Keyword:* Supercapacitor, Iron-Based Compounds, Electrochemical performance, Electrode materials

## 1. Introduction

Energy and environment have long been the main theme of today's society. Energy and the survival and development of human society are closely linked, and energy shortage is also a thorny problem. Therefore, solving energy shortage is a challenge for the entire scientific community while protecting the environment [1-3]. The relationship between chemical power and energy is getting closer and closer. Various types of fuel cells and high-energy batteries play an increasing role in human society [4-7]. Supercapacitors with high specific energy, long service life, no memory effect, and fast charging are considered to be an ideal energy storage elements as an important chemical power source [8-15].

In this paper, iron-based compounds were obtained by adding tetrabutyl titanate to ammonium fluoride system, sulfosalicylic acid system and ammonium fluoride system. The morphology was characterized by SEM. The electrode material is mixed with Super P to obtain the working electrode, and the electrochemical properties of the samples like cyclic voltammetry (CV) and galvanostatic (GCD) were studied with a three-electrode system. Then compare the common points and differences between the materials CV and GCD to obtain an ideal electrode material.

## 2. Experiment section

### 2.1. Preparation of iron-based compounds materials

#### (1). Sulfosalicylic acid system

2.5 mmol  $\text{FeCl}_3 \cdot 6\text{H}_2\text{O}$  was configured into a solution and a 0.4 mmol 5-sulfosalicylic acid (SSA,  $\text{C}_7\text{H}_6\text{O}_6\text{S} \cdot 2\text{H}_2\text{O}$ ) solution was slowly added under magnetic stirring. The solution changed from light yellow to purple quickly. Distilled water was used to adjust the volume of the solution to 35 mL, then NaOH solution was slowly added to adjust the pH of the solution to 2.38, and finally the solution capacity to 40 mL. The mixture is continued to be stirred for 30 min and then moved into a 50 mL PTFE autoclave reactor. After sealing, the reactor is placed in a  $120 \text{ }^\circ\text{C}$  oven and reacts with 8 h. After the reaction was over, the reaction kettle was removed after cooling to room temperature naturally. The as-prepared product was separated by centrifugation and washed with deionized water and anhydrous ethanol, and dried in a vacuum oven at  $50 \text{ }^\circ\text{C}$  for 12h. The sample was marked as a.

#### (2). Ammonium fluoride system

1.0 mmol  $\text{Fe}(\text{NO}_3)_3 \cdot 9\text{H}_2\text{O}$ , 2.5 mmol urea and 1.0 mmol  $\text{NH}_4\text{F}$  were into the solution with 8.75 ml water and 8.75 ml ethanol. Then the above mixture was to a 50 ml

PTFE reaction tank. The kettle was sealed and heated to 120 °C for 5h. After cooling to room temperature naturally, the sample was washed thoroughly several times with deionized water and ethanol and then dried at 60 °C for 12 h under vacuum. The obtained intermediate was annealed in a tube furnace under an Ar atmosphere for 2h at 400 °C with the heating rate of 2 °C min<sup>-1</sup>. After the annealing process, the product was obtained and marked as b.

### (3). Ammonium fluoride plus tetrabutyl titanate system

1.0 mmol Fe(NO<sub>3</sub>)<sub>3</sub>·9H<sub>2</sub>O, 2.5 mmol urea, 0.02 mmol C<sub>16</sub>H<sub>3</sub>O<sub>4</sub>Ti and 1.0 mmol NH<sub>4</sub>F were dissolved into a solution with 8.75 ml water and 8.75 ml ethanol. And then the above mixture was transferred a 50 ml PTFE reactor tank. The kettle was sealed and heated to 120 °C for 5h. Then the same process is performed as in the second method. The sample was marked as c.

## 2.2. Characterization

The surface morphology of the electrode material was observed by scanning electron microscopy (SEM). In this paper, FEI Quanta 200 scanning electron microscopy of the United States was used with an energy dispersive spectrometer. The energy dispersive spectrometer used the interaction between the electron beam and the sample to analyze the composition of the sample.

## 2.3. Electrochemical performance tests

The electrochemical properties of the composite electrode and the assembled supercapacitor were characterized with an electrochemical working station (CHI 760E Shanghai Chenhua Instrument Technology Co. Ltd.) The electrochemical properties of the supercapacitor electrodes were tested through a three-electrode system: working electrodes coated the iron-based compounds with nickel foam. A platinum electrode was used as the counter electrode. A saturated calomel electrode was used as reference electrode respectively. The electrolyte used in this test was 2 mol L<sup>-1</sup> KOH solution. The test condition was at room temperature and atmospheric environment.

### (1). CV

The following information can be obtained by cyclic voltammetry: electrochemical performance, redox potential of the substance, reversibility of the electrochemical reaction and reaction mechanism. The reversibility of the electrode material can be determined by the symmetry of the electrode material on the image. If the image is symmetrical, the reversibility is good. The shape of cyclic voltammetry curves at different scanning rates can be used to determine the capacitance properties of

electrode materials, the reversibility of electrode faraday reaction and the specific capacity of electrode materials. The calculation formula is as follows [16-18]:

$$C_m = \frac{\int IdV}{m \times S \times \Delta V} \quad (1)$$

$\Delta V$ (V) represents the potential change during the discharge, S (V/s) is the scanning rate, I (A) is the discharge current, m (g) is the mass of active substances, and  $C_m$  (F g<sup>-1</sup>) is the specific capacitance of electrode materials.

### (2). GCD

According to the literature [19-21], researchers often use the timing potential method to test the specific capacity, cyclic stability, and specific capacitance of electrode materials at various current densities. The discharge current and discharge time can be used to calculate the specific capacity of electrode materials. In this experiment, the specific capacity of electrode material and the cyclic stability of charge and discharge material are calculated by means of constant current test under different charge and discharge current densities. The formula for calculating specific capacity based on discharge time and discharge current is as follows [22-23]:

$$C_m = \frac{I \times \Delta t}{m \times \Delta V} \quad (2)$$

In the above equation, I (A) is the discharge current;  $\Delta t$  (s) is the discharge time;  $\Delta V$  (V) is the potential window and m (g) is the mass of the active substance.

### (3). Cycling stability

The cycling stability performance test was carried out with a CT2001A LAND Cell test system (Wuhan, China). The cycling stability of the prepared iron-based compounds electrode materials were tested by continuous constant current charge-discharge test. The specific capacity retention rate was calculated after 5000 charge-discharge cycles at a certain scanning rate, so as to judge the cyclic stability of the prepared electrode material.

### (4). EIS

According to AC impedance spectra, we can know the trend of impedance changing with frequency. By fitting with the corresponding electrochemical simulation software, we can get the situation of contact resistance, double-layer capacitance reactance, diffusion resistance, electrochemical resistance and so on under a certain state of the test system. The electrochemical properties of electrode materials for supercapacitors can be

evaluated by measuring the parameters of CV, GCD, cycling stability and EIS [24-28].

### 3. Results and discussion

Fig. 1 shows the different magnifications of SEM images of iron-based compounds powder prepared by ammonium fluoride plus tetrabutyl titanate system. It can be seen that the fine structure of iron-based compounds is quasi-nanosphere architecture with a diameter of about 150-200 nm. It is basically uniform in size and good in dispersion. The surface of quasi-nanosphere is rough and many wrinkles form on it. The surface undulation increases the contact area between electrolyte ions and electrode materials in solution. This structure is suitable for the requirements of electrode materials of supercapacitors.

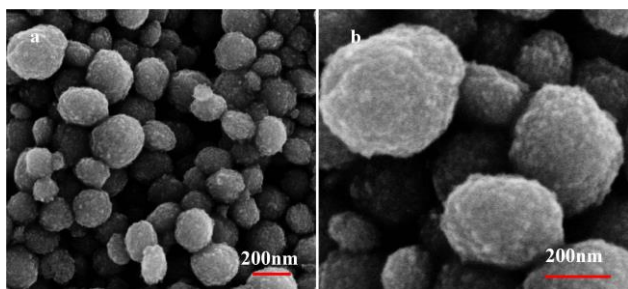


Fig. 1. Different magnifications of SEM images of iron-based compounds

The as-prepared iron-based compounds were tested as electrode materials for hybrid supercapacitors to evaluate the potential application. Fig. 2 shows the CV curves of iron-based compounds prepared by three approach electrode at the varied scan rates ranging from 5 to 60  $\text{mV s}^{-1}$  between a potential window of 0.2 and 0.6 V (vs. SCE). Every CV curve exhibits a pair of symmetric and strong redox peaks, which shows that the supercapacitor composed of electrode materials has the characteristics of pseudocapacitance and suggested that the supercapacitors electrode in this experiment have excellent reversibility and cyclic performance [29-31]. The cyclic voltammetric images of tetrabutyl titanate added to ammonium fluoride system show that redox peaks are high appear at all scanning rates and the symmetry is especially good. This indicates that reversible redox reaction occurs during the cyclic process, and further illustrates that the supercapacitors in this experiment have the characteristics of supercapacitors.

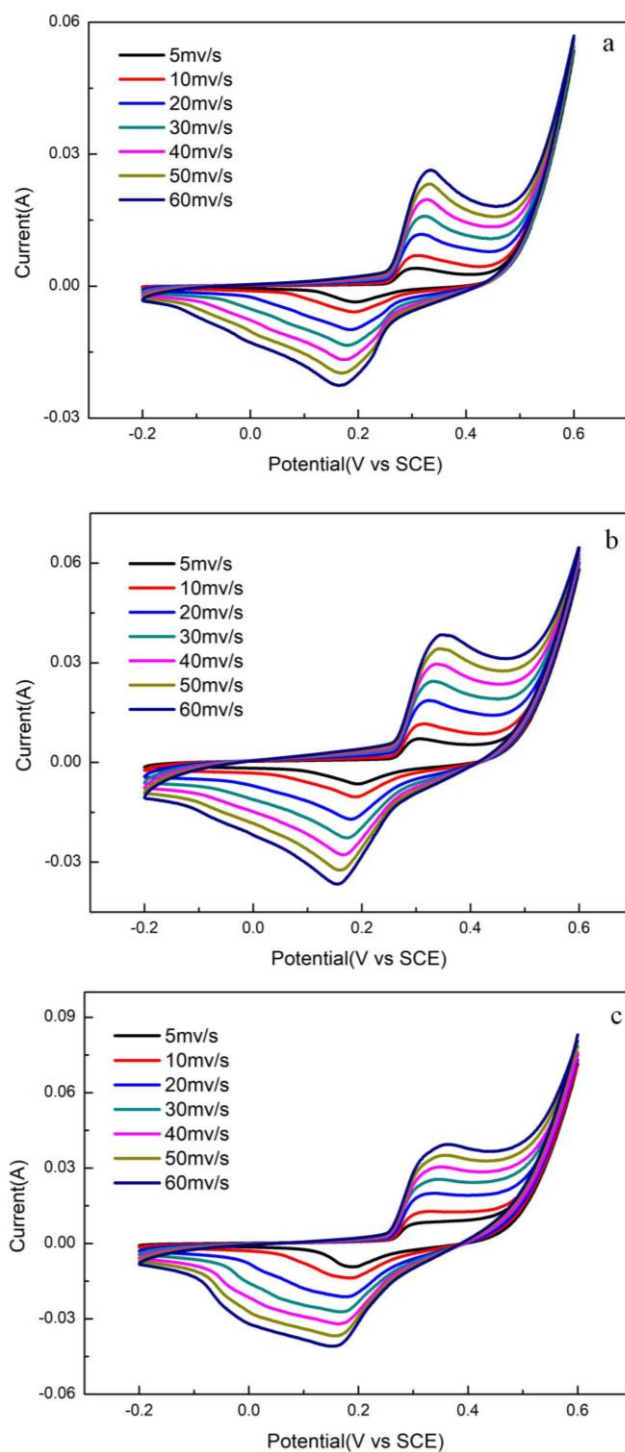


Fig. 2. Cyclic voltammetry of iron-based compounds of a) sulfosalicylic acid system; b) ammonium fluoride systems; c) tetrabutyl titanate added to ammonium fluoride system (color online)

Fig. 3 shows the charge-discharge curves of iron-based compounds electrode at the charge-discharge current densities of 1, 2, 3, 4, 5, 10 and 20  $\text{A g}^{-1}$  with a potential range from 0 to 0.45 V (vs. SCE) respectively. The charge-discharge curves show distinct plateau regions at different current densities, in accordance with the results

of CV test. The typical faradaic nature was further verified by the charge-discharge curves. For comparison, it can be seen that the supercapacitor composed of iron-based compounds synthesized by adding tetrabutyl titanate to ammonium fluoride system in Fig. 3 c) has a longer charge-discharge time and a wider charge-discharge platform under the same current density. The iron-based compounds material synthesized in this system may be widely used in near future as electrode material for supercapacitors.

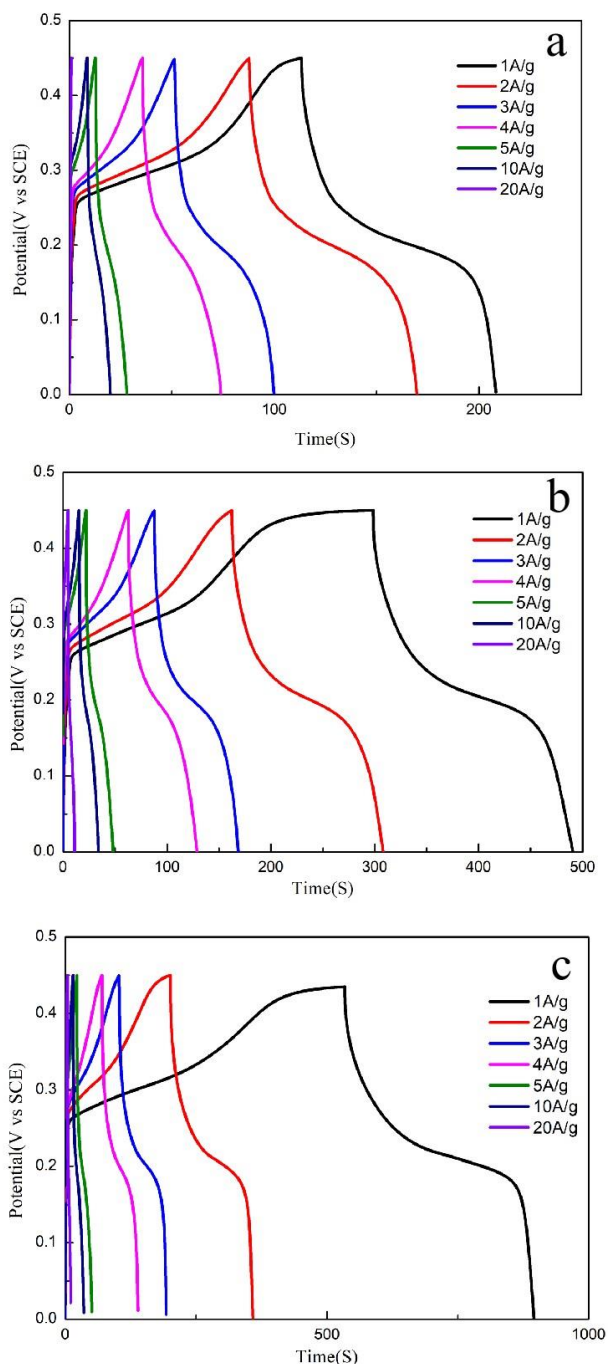


Fig. 3. Constant current charge-discharge image of iron-based compounds a) sulfosalicylic acid system; b) ammonium fluoride system; c) tetrabutyl titanate added to ammonium fluoride system (color online)

The calculated specific capacitance values of samples at the charge-discharge current densities of 1, 2, 3, 4, 5, 10 and 20  $\text{A g}^{-1}$  are shown in Fig. 4 (a). According to the experimental results, the maximum specific capacities of the prepared materials are 830  $\text{F g}^{-1}$  for ammonium fluoride with tetrabutyl titanate system (sample c), 430  $\text{F g}^{-1}$  for ammonium fluoride system (sample b) and 210  $\text{F g}^{-1}$  for sulfosalicylic acid system (sample a) at 1  $\text{A g}^{-1}$ . It can be seen that sample a has the lowest specific capacity among all the samples. For sample b, the specific capacitance values are more than the sample a. Encouragingly, sample c exhibits highest specific capacitances of 830, 700, 650, 609, 508, 462 and 405  $\text{F g}^{-1}$  at the discharge current densities of 1, 2, 3, 4, 5, 10 and 20  $\text{A g}^{-1}$ , respectively, suggesting a good rate performance. It can be concluded that the specific capacitance of iron-based compounds material can be increased by adding fluorine and titanium in the synthesis system. The reason may be that the conductivity of the material is improved by adding fluorine and titanium.

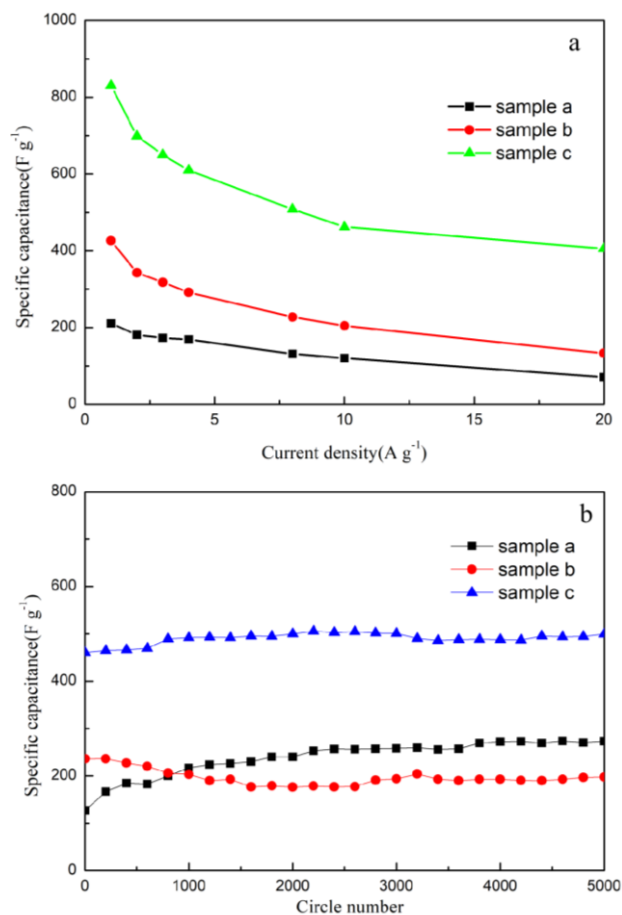


Fig. 4. relationship between specific capacity and current density; b) Cycling performance of samples at a current density of 10  $\text{A g}^{-1}$  (color online)

As known, cycling stability is a very important parameter for electrode material. For samples, Fig. 4 (b) shows their cycling stability evaluated by repeated GCD measurement at a current density of  $10 \text{ A g}^{-1}$ . For sample a, the capacitance continuously increases in the initial cycles and then stays constant. In the case of sample b, it decreases slightly at first and then remains constant. While for sample c, the performance has been stable until 5000 cycles and retains around  $500 \text{ F g}^{-1}$  at  $10 \text{ A g}^{-1}$ . So sample c demonstrates very good cycling stability.

The iron-based compounds material synthesized by adding tetrabutyl titanate to ammonium fluoride has a relatively fast exchange rate between electrons and ions, which directly affects the charging and discharging rate of the supercapacitor and the specific capacity of the supercapacitor in a certain period of time. Therefore, the specific capacity is larger than that of other materials. It is proved that it is larger than capacitance at the same current density [32-33]. Iron-based materials are widely used in the field of energy storage [34-36], and the obtained iron-based materials in this work exhibit potential as electrode materials of supercapacitor.

#### 4. Conclusion

In this work, iron-based compounds were prepared by changing the composition of the solution in the simple hydrolysis process. The iron-based compound material synthesized with ammonium fluoride and tetrabutyl titanate system exhibited the highest specific capacity and best cycling stability. The specific capacity of material is  $830 \text{ F g}^{-1}$  at  $1 \text{ A g}^{-1}$  and the efficiency of cycling stability remains at almost 100% after cycling 5000 times at a current density of  $10 \text{ A g}^{-1}$ .

#### Acknowledgements

This work was supported by Shandong Provincial Natural Science Foundation (ZR2019MB071) and the Key Research and Development Program of Shandong Province (2019GGX103011), National Undergraduate Training Program for Innovation and Entrepreneurship (201710449019) and Student Research Training Program of Binzhou University (SRTP2019212).

#### References

- [1] C. C. Hou, Q. Li, C. J. Wang, C. Y. Peng, Q. Q. Chen, H. F. Ye, W. F. Fu, C. M. Che, N. López, Y. Chen, *Energy Environ. Sci.* **10**, 1770 (2017).
- [2] L. Ye, L. Zhao, H. Zhang, B. Zhang, H. Wang, J. *Mater. Chem. A* **4**, 9160 (2016).
- [3] Y. Lu, J. Liu, X. Liu, S. Huang, T. Wang, X. Wang, C. Gu, J. Tu, S. X. Mao, *CrystEngComm.* **15**, 7071 (2013).
- [4] M. Yu, Y. Zeng, Y. Han, X. Cheng, W. Zhao, C. Liang, Y. Tong, H. Tang, X. Lu, *Adv. Funct. Mater.* **25**, 3534 (2015).
- [5] Y. Wang, Y. Song, Y. Xia, *Chem. Soc. Rev.* **45**, 5925 (2016).
- [6] J. Gou, S. Xie, Y. Liu, C. Liu, *Electrochim. Acta* **210**, 915 (2016).
- [7] S. Hou, X. Xu, M. Wang, Y. Xu, T. Lu, Y. Yao, L. Pan, *J. Mater. Chem. A* **5**, 19054 (2017).
- [8] S. Xie, J. Gou, *J. Alloy. Compd.* **713**, 10 (2017).
- [9] X. Zhang, L. Huang, Q. Wang, S. Dong, *J. Mater. Chem. A* **5**, 18839 (2017).
- [10] J. Gou, *J. Electrochem. Soc.* **164**, A3326 (2017).
- [11] J. Zhao, Y. Li, G. Wang, T. Wei, Z. Liu, K. Cheng, K. Ye, K. Zhu, D. Cao, Z. Fan, *J. Mater. Chem. A* **5**, 23085 (2017).
- [12] J. Gou, *New J. Chem.* **42**, 7138 (2018).
- [13] X. Liang, K. Chen, D. Xue, *Adv. Energy Mater.* **8**, 1703329 (2018).
- [14] Xue Dongfeng, Chen Kunfeng, *Mater. Res. Bull.* **83**, 201 (2016).
- [15] K. Chen, D. Xue, *The Chemical Record* **18**, 282 (2018).
- [16] J. Yu, Q. Li, Y. Li, C. Y. Xu, L. Zhen, V. P. Dravid, J. Wu, *Adv. Funct. Mater.* **26**, 7644 (2016).
- [17] Q. Qin, J. Liu, W. Mao, C. Xu, B. Lan, Y. Wang, Y. Zhang, J. Yan, Y. Wu, *Nanoscale* **10**, 7377 (2018).
- [18] J. Lin, H. Jia, H. Liang, S. Chen, Y. Cai, J. Qi, C. Qu, J. Cao, W. Fei, J. Feng, *Chem. Eng. J.* **336**, 562 (2018).
- [19] S. Xie, J. Gou, B. Liu, C. Liu, *Inorg. Chem. Front.* **5**, 1218 (2018).
- [20] J. Song, C. Zhu, B.Z. Xu, S. Fu, M. H. Engelhard, R. Ye, D. Du, S. P. Beckman, Y. Lin, *Adv. Energy Mater.* **7**, 1601555 (2016).
- [21] P. He, X. Y. Yu, X.W. Lou, *Angew. Chem. Int. Ed. Engl.* **56**, 3897 (2017).
- [22] F. X. Ma, L. Yu, C. Y. Xu, X. W. Lou, *Energ. Environ. Sci.* **9**, 862 (2016).
- [23] Z. Wu, J. Guo, J. Wang, R. Liu, W. Xiao, C. Xuan, K. Xia, D. Wang, *ACS Appl. Mater. Inter.* **9**, 5288 (2017).
- [24] Y. M. Chen, Z. Li, X. W. Lou, *Angew. Chem.* **127**, 10667 (2015).
- [25] J. Kibsgaard, C. Tsai, K. Chan, J. D. Benck, J. K. Nørskov, F. Abild-Pedersen, T. F. Jaramillo, *Energ. Environ. Sci.* **8**, 3022 (2015).
- [26] D. R. Liyanage, S. J. Danforth, Y. Liu, M. E. Bussell, S. L. Brock, *Chem. Mater.* **27**, 4349 (2015).
- [27] E. A. A. Aboelazm, G. A. M. Ali, H. Algarni, H. Yin, Y. L. Zhong, K. F. Chong, *J. Phys. Chem. C* **122**, 12200 (2018).
- [28] C. Wang, J. Jiang, T. Ding, G. Chen, W. Xu, Q. Yang, *Adv. Mater. Interfaces* **3**, 1500454 (2016).
- [29] Y. Tan, H. Wang, P. Liu, Y. Shen, C. Cheng, A. Hirata, T. Fujita, Z. Tang, M. Chen, *Energy Environ. Sci.* **9**, 2257 (2016).
- [30] R. Ye, P. del Angel-Vicente, Y. Liu, M. J.

- Arellano-Jimenez, Z. Peng, T. Wang, Y. Li, B. I. Yakobson, S.-H. Wei, M. J. Yacaman, J. M. Tour, *Adv. Mater.* **28**, 1427 (2016).
- [31] Y. Liu, N. Fu, G. Zhang, M. Xu, W. Lu, L. Zhou, H. Huang, *Adv. Funct. Mater.* **27**, 1605307 (2017).
- [32] J. Gou, S. Xie, Z. Yang, Y. Liu, Y. Chen, Y. Liu, C. Liu, *Electrochim. Acta* **229**, 299 (2017).
- [33] M. J. Deng, C. Z. Song, C. C. Wang, Y. C. Tseng, J. M. Chen, K. T. Lu, *ACS Appl. Mater. Interfaces* **7**, 9147 (2015).
- [34] K. Chen, Y. D. Noh, W. Huang, J. Ma, S. Komarneni, D. Xue, *Ceram. Int.* **40**, 2877 (2014).
- [35] X. Chen, K. Chen, H. Wang, S. Song, D. Xue, *CrystEngComm.* **16**, 6707 (2014).
- [36] M. Zhang, K. Chen, X. Chen, X. Peng, X. Sun, D. Xue, *CrystEngComm.* **17**, 1917 (2015).

---

\*Corresponding author: shenglixie@126.com,  
goujianxia@163.com